

Quantum Nonlocality in Two-Photon Experiments at Berkeley

Raymond Y. Chiao†, Paul G. Kwiat‡ and Aephraim M. Steinberg§

† Department of Physics, University of California, Berkeley, CA 94720-7300, U.S.A.

‡ Institut für Experimentalphysik, Universität Innsbruck, Technikerstrasse 25, A-6020 Innsbruck, Austria

§ National Institute of Standards and Technology, Phys A167, Gaithersburg, MD 20899, U.S.A.

(Preprint quant-ph/9501016; This version was produced on December 21, 1994)

We review some of our experiments performed over the past few years on two-photon interference. These include a test of Bell's inequalities, a study of the complementarity principle, an application of EPR correlations for dispersion-free time-measurements, and an experiment to demonstrate the superluminal nature of the tunneling process. The nonlocal character of the quantum world is brought out clearly by these experiments. As we explain, however, quantum nonlocality is not inconsistent with Einstein causality.

I. INTRODUCTION

We shall begin with a brief review of the Einstein-Podolsky-Rosen (EPR) “paradox” [1], and then review some of our experiments at Berkeley: the Franson experiment [2,3], the “quantum eraser” [4], the “dispersion-cancellation” effect [5], and tunneling-time measurements [6,7]. Let us begin by stating that we consider the EPR phenomenon to be an “effect,” not a “paradox”: EPR's experimental predictions are internally consistent, and a contradiction is only reached if one assumes both EPR's notion of locality and the completeness of quantum mechanics (QM). The three central elements that constitute the EPR argument are 1) a belief in some of the quantum-mechanical predictions concerning two separated particles, 2) a very reasonable definition of an “element of reality” [namely, that “if, without in any way disturbing a system, we can predict with certainty (i.e., with probability equal to unity) the value of a physical quantity, then there exists an element of physical reality corresponding to this physical quantity”], and 3) a belief that nature is local, i.e., that no expectation values at a spacetime point x_2 can depend on an event at a spacelike-separated point x_1 (this definition of locality is now seen to be more stringent than Einsteinian causality, and is inconsistent with QM). In the original EPR scheme [1], the system under consideration is a pair of particles described by the wavefunction $\delta(x_1 - x_2 - a)$. This is a simultaneous eigenstate of the operator $(X_1 - X_2)$ [with eigenvalue a], and the operator $(P_1 + P_2)$ [with eigenvalue 0], which is possible since the commutator $[X_1 - X_2, P_1 + P_2]$ vanishes. In other words, the *sum* of the particles' momenta is well-defined, as is the *difference* of their positions. Therefore, if we measure the momentum of one particle, we can predict with certainty the momentum of the other (hypothesis 1), even though it may be sufficiently far away that no signal could be transferred between them (hypothesis 3). Momentum must therefore be an element of reality (hypothesis 2). And if we measure the position of one, then we can predict with certainty the position of the other (possibly distant) particle. Hence, position is also an element of reality. But quantum mechanics does not allow a precise specification of both the position and the momentum of a particle. This was not a paradox to EPR; rather, they concluded that quantum mechanics must be incomplete—a complete theory would not contradict the predictions of QM, but would incorporate all elements of reality, just as atomic theory incorporates the positions and momenta of individual atoms, variables not described by thermodynamics.

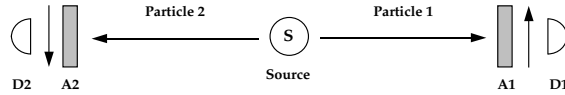


FIG. 1. Bohm's version of the EPR Gedankenexperiment

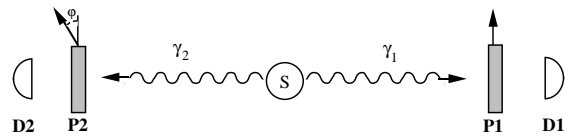


FIG. 2. Optical version of EPR experiment

In Bohm's version of the EPR effect [8], (see Fig. 1) a spin-0 particle decays into two spin-1/2 particles in the singlet state

$$|\text{Singlet}\rangle = \frac{1}{\sqrt{2}}\{|\uparrow_1\rangle|\downarrow_2\rangle - |\uparrow_2\rangle|\downarrow_1\rangle\}. \quad (1)$$

The filters A1 and A2 in Fig. 1 are Stern-Gerlach apparatuses. Optical versions of this experiment performed by Freedman and Clauser, and by Aspect *et al.*, used photons in place of the spin-1/2 particles, and linear polarizers (P1, P2) in place of Stern-Gerlach apparatuses [9–11]; see Fig. 2. The coincidence count rate as a function of the relative angle between polarizers P1 and P2 is a measure of the correlated behavior of the two separated particles. Bell derived an inequality [12] starting from EPR’s very general and seemingly reasonable notions of locality and realism; this inequality is violated by the high-visibility sinusoidal fringes predicted by quantum mechanics. Most importantly, *experiments* yield results in agreement with quantum mechanics, and in violation of this inequality (modulo some reasonable auxiliary assumptions about uncounted particles). Therefore, these experiments rule out a broad class of local realistic theories.

These early experiments relied on the correlations of the polarization (i.e., *internal* degrees of freedom) of the particles. Since the predictions of quantum mechanics are so strange, it is important to investigate them for *external* degrees of freedom as well, such as the momentum and position of the particles considered in the original EPR paper. Rarity and Tapster have already done so for momentum and position [13], and recently we have performed an experiment [3] (first proposed by Franson [2]) relying on the external variables of energy and time.

II. ENTANGLED STATES

Erwin Schrödinger [14], in response to the EPR paper, pointed out that at the heart of these nonlocal effects is what he called “entangled states” in quantum mechanics, i.e., *nonfactorizable* superpositions of product states. For if a two-particle wavefunction were factorizable,

$$\psi(x_1, x_2) = \chi(x_1)\chi(x_2) \quad (2)$$

then the probability of joint detection would also factorize,

$$|\psi(x_1, x_2)|^2 = |\chi(x_1)|^2|\chi(x_2)|^2 \quad (3)$$

so that the outcomes of two spatially separated measurements would be *independent* of one another. In cases where the two-particle state cannot be factorized as above, this means that the quantum-mechanical prediction implies nonlocal correlations in the behavior of remote particles. The Bohm singlet state (1) is such an entangled state. It predicts correlations between spin measurements made on the two particles. But these correlations persist even if the particles and their analyzers are separated by space-like intervals, implying the existence of non-local influences. Though each particle considered individually is unpolarized, the two particles will *always* have opposite spin projections when measured along the same quantization axis. Einstein *et al.* would conclude that each spin component is an “element of reality” in that it would be possible to predict its value with 100% certainty without disturbing the particle, simply by measuring the corresponding spin component of the particle’s twin (a measurement which according to EPR’s locality hypothesis cannot disturb the particle in question). As discussed above, this reasoning led EPR to conclude that quantum mechanics was incomplete; if one instead considers QM to be a complete theory, one must then admit the existence of nonlocal effects. As we shall see below, experiment supports this latter interpretation.

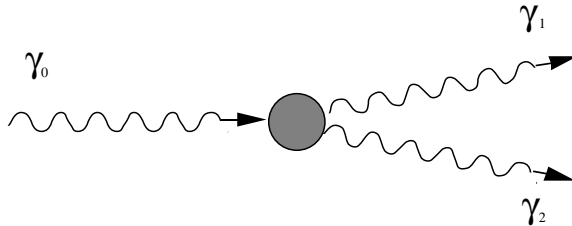


FIG. 3. Two-photon decay from one photon

In our experiments, the entangled state we start with is the *energy-entangled* state of two photons produced in a two-photon decay process known as spontaneous parametric fluorescence. The Feynman diagram for this process is shown in Fig. 3, and the state of the two-photon system after decay from a parent photon with a sharply defined energy E_0 is given by

$$|2 \text{ photons} \rangle = \int_0^{E_0} \int_0^{E_0} dE_1 dE_2 \delta(E_0 - E_1 - E_2) A(E_1, E_2) |E_1 \rangle |E_2 \rangle . \quad (4)$$

Instead of a sum, as in the singlet state, we now have an integral, since energy is a continuous variable. The meaning of this energy-entangled state is that after the measurement of one photon's energy gives the sharp value E_1 , there is an instantaneous “collapse” to the state

$$|E_1 \rangle |E_0 - E_1 \rangle . \quad (5)$$

This effect has been seen in an earlier experiment [15], in which coincidences were recorded between photon γ_1 , which passed through an interference filter (to measure its frequency, and hence its energy, with high resolution) and photon γ_2 , which passed through a Michelson interferometer (to measure its width); when photon γ_1 was detected after the narrow-band filter, photon γ_2 collapsed into an equally narrow-band energy state, whose coherence length was then far greater than that of the uncollapsed state.

III. THE TWO-PHOTON LIGHT SOURCE

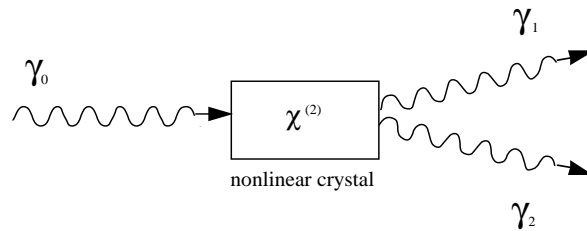


FIG. 4. Parametric down-conversion

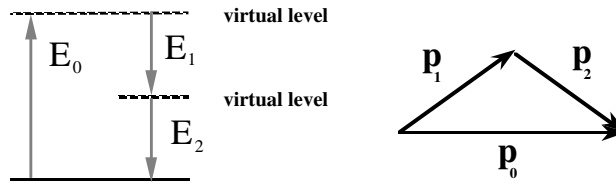


FIG. 5. Energy level diagram; momentum conservation triangle

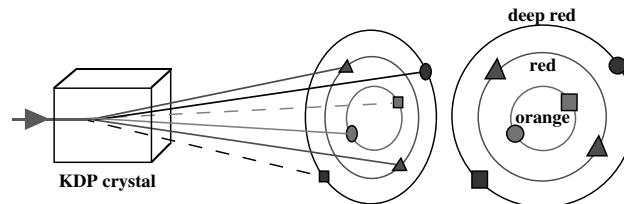


FIG. 6. Parametric down-conversion process. Matching shapes represent conjugate photons, while each ring represents a different color.

The two-photon decay, or parametric down-conversion, occurs inside a crystal with a $\chi^{(2)}$ nonlinearity (we used a potassium dihydrogen phosphate (KDP) crystal). This process is the reverse of second harmonic generation, in which two red photons combine to form an ultraviolet photon at twice the frequency. In our crystal, a single photon γ_0 produced by a cw ultraviolet laser (a single-mode argon ion laser at 351 nm) down-converts to two red photons γ_1 and γ_2 , each near 702 nm. Energy and momentum are conserved here:

$$\begin{aligned} E_0 &= E_1 + E_2 \\ \mathbf{p}_0 &= \mathbf{p}_1 + \mathbf{p}_2 . \end{aligned} \quad (6)$$

The parent photon γ_0 is called the “pump” photon, daughter photon γ_1 the “signal” photon, and daughter photon γ_2 the “idler” photon, for historical reasons. A rainbow of colored cones (see Fig. 6) is produced around an axis defined by the UV laser beam, where any two correlated photons will lie on opposite sides of the cone, e.g., the inner “square” orange photon is conjugate to the outer “square” deep-red photon, etc. The two conjugate photons are always produced essentially simultaneously in the two-photon decay: They have been observed to be born within tens of femtoseconds of each other. Though due to the continuous-wave nature of the pump laser, no expectation values of this source are time-dependent, the photon correlations mean that once one particle is detected, the other collapses into a very short wavepacket. The wavepacket is narrow because there are many ways to partition the energy of the parent photon, so that each daughter photon has a broad spectrum. However, due to the entanglement [described by the state (4)], the sum of the two photons’ energies is extremely well-determined. Thus, the *sum* of their energies and the *difference* of their arrival times can be simultaneously known to high precision, though the absolute time of emission is unknown. This is to be contrasted with the case of the single particle, whose time and energy may not be known to arbitrary accuracy due to the uncertainty principle; hence the correlations are of the exact sort Einstein *et al* used to argue that quantum mechanics must be incomplete.

IV. THE FRANSON EXPERIMENT

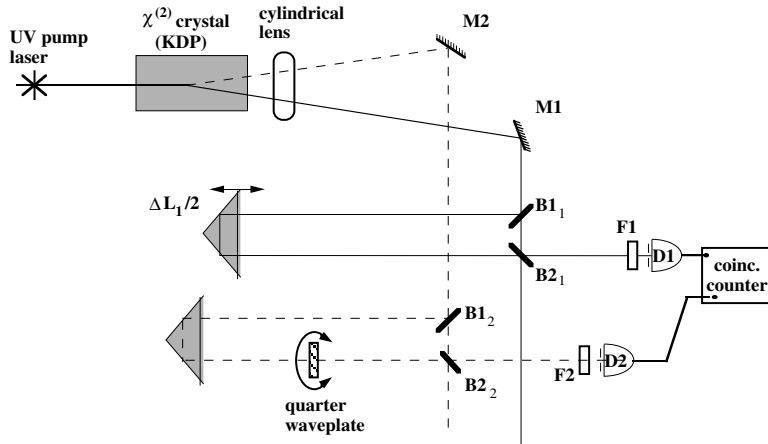


FIG. 7. Apparatus used at Berkeley to perform the Franson experiment

The Franson experiment [2] allows an examination of Bell’s inequality for energy and time, a violation of which implies that photons do not necessarily possess a well-defined energy nor a well-defined time of emission before measurement. Our experiment [3] is sketched in Fig. 7. (Similar experiments were performed by Brendel *et al* [16], and by Rarity and Tapster [17].) The correlated photons are directed to two separate but identical Mach-Zehnder-like interferometers, in which they are allowed to take either a short path or a long path. These interferometers can have their path-length differences adjusted by means of trombone prisms in their long paths and a waveplate in that of interferometer 2.

There is no first-order interference inside a single interferometer, because the coherence lengths of the photons ($\sim 50 \mu\text{m}$) are much smaller than the 63-cm path-length differences in the interferometers. However, there is second-order (i.e., two-photon) interference observable in coincidence detection between detectors D1 and D2. We shall use Feynman’s rules for interference to calculate the probability of coincidence detection. The indistinguishable processes here are (1) the “short-short” and (2) the “long-long” processes (where both photons take their interferometers’ short or long paths, respectively). The distinguishable processes are (3) the “short-long” and (4) the “long-short” processes, since the delays between the “clicks” of D1 and D2 differentiate these events from one another, as well as from processes (1) and (2). In principle and also in practice, we are able to reject these distinguishable “clicks” by using a sufficiently narrow coincidence timing window in our electronics. We are thus left with only the two indistinguishable processes (1) and (2), for which we must first add the probability *amplitudes*, and then take the absolute square. Hence the probability of a given coincidence detection is given by the expression

$$P_c \propto |1 \cdot 1 - e^{i\phi_1} \cdot e^{i\phi_2}|^2 \propto [1 - \cos(\phi_1 + \phi_2)] , \quad (7)$$

where the first term inside the absolute value corresponds to the “short-short” process, and the second term to the “long-long” process. (The beam splitters are assumed to be 50/50 throughout, and a $\pi/2$ phase shift for reflection is assumed.) Here the phases ϕ_1 and ϕ_2 represent the phase differences between the short and long arms of interferometers 1 and 2, respectively.

Note that equation (7) implies a fringe visibility of 100%, i.e., perfect zeros at the minima in coincidence detection. The meaning of these minima is that the two spatially separated photons behave in an *anticorrelated* fashion: if one is transmitted at the final beam splitter, then the other is reflected. The meaning of the maxima of equation (7) is that the two photons behave in a *correlated* fashion: either both are transmitted at the final beam splitter, or both are reflected. The behavior of the twins depends on the settings of the separate phase shifters; the phases in our experiment were varied continuously, using a piezo-electrically driven trombone arm in one interferometer (ϕ_1), as well as discretely in increments of 90° , using a quarter waveplate in the other interferometer (ϕ_2). Note that in principle the phases could even be set *after* the photons had entered the interferometers.

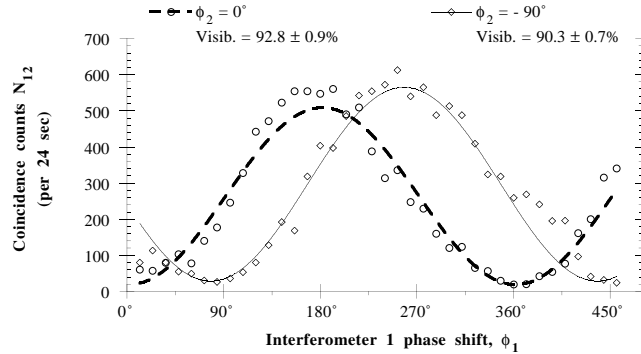


FIG. 8. Interference fringes of our Franson experiment, for different phase settings of the quarter waveplate: $\phi_2 = -90^\circ$ (\diamond); $\phi_2 = 0^\circ$ (\circ)

In Fig. 8 we present our latest data. The mere existence of interference fringes means that one cannot know, even in principle, the actual emission times of the photons, for otherwise their arrival times at the detectors would indicate whether the long or short paths had been taken, and there would no longer be two interfering processes (see the following section). Bell’s inequality for this experiment is violated by fringes which vary sinusoidally with $\phi_1 + \phi_2$ and have visibility greater than 70.7% ($= 1/\sqrt{2}$), once certain reasonable assumptions about uncounted photons are made. In our experiment, we observed fringes with the expected dependence only on the sum of the phases, with visibilities exceeding the limit by as many as 28 standard deviations. Using a “fair-sampling” assumption and the symmetry properties of the interferometer (in particular, that the coincidence rate of the unused ports in Fig. 7 is equal to that of the used ports, an assumption supported by tests done with a third detector not shown in the figure), we can directly obtain the value of the Bell-parameter S from the coincidence rates obtained at two values each of ϕ_1 and ϕ_2 . S is a measure of the strength of the correlations between the two particles, evaluated for the four combinations of the two values of ϕ_1 and ϕ_2 , and according to the Clauser-Horne-Shimony-Holt form of Bell’s inequality [18], satisfy $|S| \leq 2$ for any local realistic model. For appropriate choices of ϕ_1 (45° and 135°) and ϕ_2 (0° and -90°), we obtain $S = -2.63 \pm 0.08$, clearly displaying quantum nonlocality [19].

V. THE “QUANTUM ERASER”

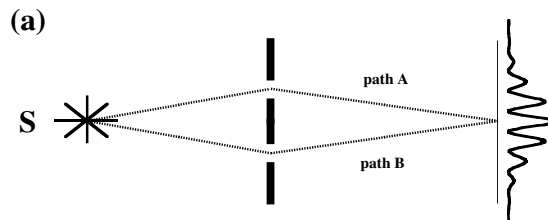


FIG. 9. (a) Young’s two-slit experiment, (b) with circular polarizers, (c) with circular polarizers and linear polarizer; for latex reasons temporarily beyond our control, b and c removed

Although the nonlocality of quantum mechanics is most apparent in tests of Bell’s inequalities, it also plays a central role in experiments exploring complementarity. One such, the “quantum eraser,” was discussed by Scully, Englert and Walther [20] in connection with the micromaser. In Fig. 9 we first present a simple precursor to this idea. Consider Young’s two-slit experiment from a particle viewpoint. The reason we see interference at the screen in Fig. 9 (a) is that one cannot know, *even in principle*, which path (A or B) the particle took on its way to the screen. This lack of which-path information is fundamental to the observability of interference fringes. However, suppose we placed two circular polarizers of opposite senses, CP1 and CP2, in front of the two slits, as shown in Fig. 9 (b). The photons which have passed through these circular polarizers are now *labeled* by their polarizations, so that by measuring their helicities, one could tell which path the photons took to the screen. Hence we shall call these polarizers “labelers.” Since we now have which-path information, the interference pattern on the screen disappears; half the time, the diffraction pattern of slit 1 appears, and half the time the diffraction pattern of slit 2 appears, but since these two processes are made mutually exclusive by the which-path labels, no interference occurs between them. (Note that the center-of-mass motion of the particles is in no way disturbed in the transverse directions by the insertion of the circular polarizers, so that this scheme is very different from Feynman’s [21], where due to the uncertainty principle, the scattering of a particle near one of the slits uncontrollably disturbs the transverse center-of-mass motion. However, Stern *et al* [22] have proved that the presence of a which-path detector in an interferometer always leads to a random phase shift, thus washing out the interference fringes.) Now let us “erase” the which-path information by the insertion of a linear polarizer LP in front of the screen; see Fig. 9 (c). The linear polarizer erases the handedness of the photons, which served as their labels. (Note that the orientation of the axis of this linear polarizer is immaterial for this erasure to occur; it only affects the phase of the resulting interference pattern.) Since which-path information is no longer available, the interference pattern is revived.

FIG. 10. Figure temporarily unavailable. Hong-Ou-Mandel interferometer; resulting coincidence dip.

This particular version of the quantum eraser has a straightforward classical-wave explanation when the light source is describable in terms of coherent states. Thus it could be argued that there is nothing particularly quantum about this quantum eraser. Nevertheless, Jordan has proposed a similar Mach-Zehnder version of this experiment [23], in which he has argued on the basis of the correspondence principle that despite the existence of a classical explanation, such first-order interference experiments can be interpreted as true quantum erasers. However, in order to avoid any possible ambiguity concerning the quantum versus classical interpretation, we decided to use the nonclassical two-photon light source described above, in conjunction with the Hong-Ou-Mandel (HOM) two-photon interferometer [24], to demonstrate a quantum eraser with no classical analog. Due to the use of single particles, the meaning of which-path information is clear, whereas in a classical-wave experiment, it is questionable whether there is any way to ask which path a wave took. In the interferometer shown in Fig. 10, the two twin photons are brought back together by means of mirrors, so that they impinge simultaneously on a 50/50 beam splitter, after which they continue on to the two detectors D1 and D2. The coincidence rate recorded by these detectors is observed to go through a sharp dip as the path length difference between the two photons is varied. The width of this dip in our experiments is typically $\lesssim 100$ femtoseconds, allowing very high resolution in time-of-flight comparisons between the two photons, as we shall discuss in detail in sections VI and VII.

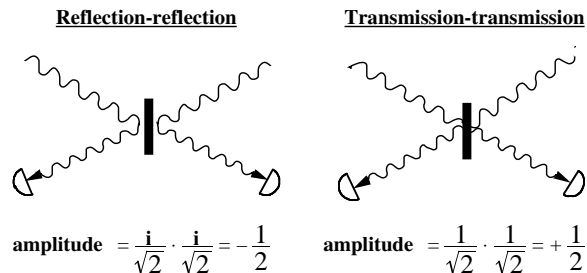


FIG. 11. The two indistinguishable processes leading to coincidences

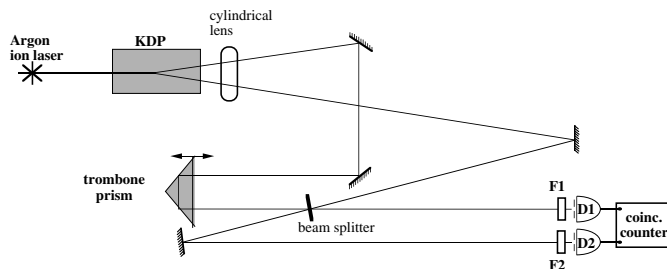


FIG. 12. Hong-Ou-Mandel interferometer (Berkeley version)

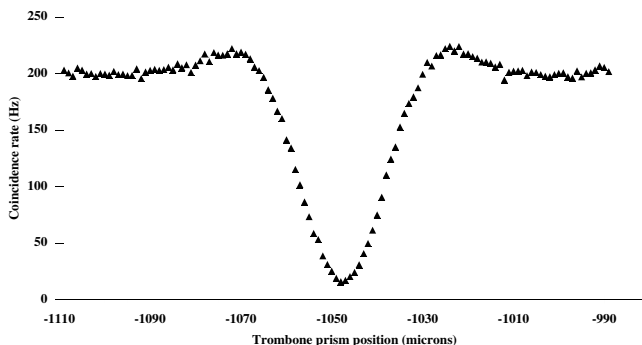


FIG. 13. Coincidence rate versus trombone prism position

To explain this effect, we again employ Feynman’s rules for interference. The possible processes for the two photons at the beam splitter are:

- (1) Both photons are transmitted; the outcome— a coincidence “click” of D1 and D2.
- (2) and (3) One photon is reflected, the other transmitted; the outcome— no coincidences.
- (4) Both photons are reflected; the outcome— a coincidence “click” of D1 and D2.

If the two photons reach the beam splitter simultaneously, coincidence detection processes (1) and (4) are indistinguishable, and thus interfere; see Fig. 11. The phase factor i for the reflection amplitude (relative to its transmission amplitude) arises from time-reversal symmetry at a lossless, symmetric beam splitter [25], and results in destructive interference of the “reflection-reflection” and “transmission-transmission” probability amplitudes. Hence the total amplitude for coincidences to occur is $(1^2/2 + i^2/2) = 0$: Coincidences never occur. In other words, the two photons always exit the same port of the beam splitter whenever the path length difference is zero, i.e., if the photon wavepackets arrive at the beam splitter *simultaneously*. However, processes (1) and (4) become distinguishable if the photon wavepackets arrive at different times at the beam splitter, and coincidences then occur half the time. Hence as the path length difference is scanned, one maps out the overlap of the photon wavepackets; the width of the coincidence dip is a measure of the coherence length of the single-photon wavepackets. A schematic of our version of the HOM interferometer is shown in Fig. 12. A typical coincidence dip is shown in Fig. 13.

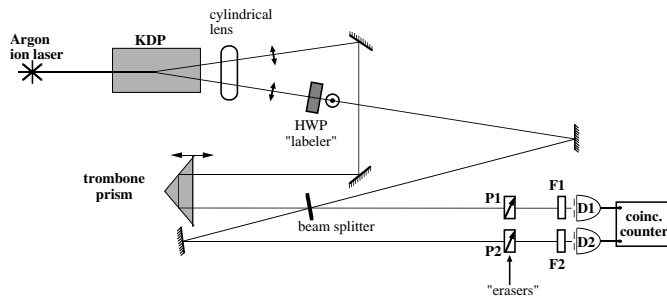


FIG. 14. Hong-Ou-Mandel interferometer with “labeler” and “erasers”

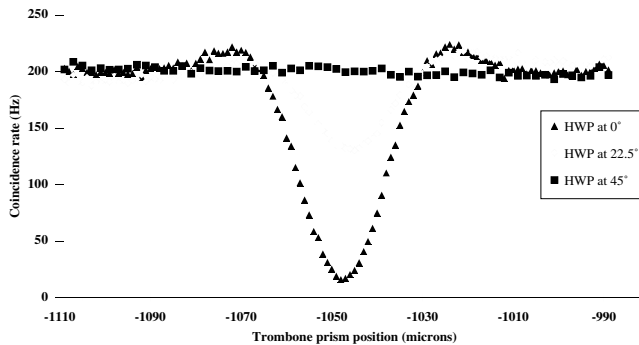


FIG. 15. Coincidence rate versus trombone prism position with “labeler” in setup, but without “erasers”

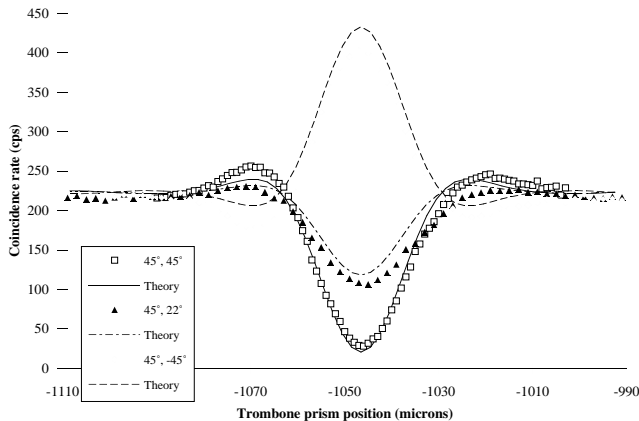


FIG. 16. Revival of interference due to (partial) erasure, for different polarizer settings indicated in the legend.

As in the simpler Young’s-type experiment described earlier, in our version of the quantum eraser we used polarization as a means of labeling the photons. The two twin photons emerge from our nonlinear crystal horizontally polarized. We now add to one arm of the interferometer a half-wave plate (HWP), which can rotate the photon’s polarization to vertical. This clearly gives information on which path the photon takes, thereby distinguishing the otherwise interfering “reflection-reflection” and “transmission-transmission” processes. In Fig. 15 we show the disappearance of the coincidence dip, as we rotate the the fast axis of the half-wave plate towards 45° with respect to the horizontal, at which point the polarizations of the down-converted photons are orthogonal, and the previously interfering paths fully distinguishable. (An intermediate orientation of the half-wave plate is also shown.) Now we put in the erasers, which take the form of two linear polarizers, P1 and P2, in front of the detectors. By orienting both of them at 45° to the horizontal, we can erase the which-path information, since both horizontally and vertically polarized photons end up polarized at 45° after passing through these polarizers, and any possibility of distinguishing between the paths taken by the photons is lost. The result is that the interference pattern, i.e., the coincidence dip, is now revived, as shown by the data represented by the squares of Fig. 16. Note that the presence of *both* polarizers P1 and P2 is necessary to perform the erasure. The removal of either one would leave *one* of the photons labeled, carrying enough which-path information to totally destroy the interference pattern. We stress that it is the mere *possibility* of obtaining which-path information that destroys the interference; no actual polarization measurements need to be made. An interesting feature of this experiment is that one can change the coincidence dip into a coincidence peak (i.e., an interference minimum into a maximum), by rotating P1 relative to P2 until one is at $+45^\circ$ and the other is at -45° . The data for this orientation are represented by the diamonds in Fig. 16; an intermediate orientation is also shown. (We have also checked that the coincidence rate at the center of the dip varies sinusoidally with the *relative* angle of P1 and P2, which Shih & Alley and Ou & Mandel have already observed in connection with Bell’s inequality experiments [26,27]). In an advanced version of the quantum eraser experiments, it should even be possible to incorporate a “delayed choice” feature [28], so that the choice of observing fringes and anti-fringes or retaining which-way information is made *after* the initially interfering particle is detected [29].

VI. DISPERSION CANCELLATION IN TWO-PHOTON INTERFERENCE

As a motivation for the next experiment, involving dispersion cancellation, let us return for a moment to the classical problem of propagation in a dispersive medium. We know that the peak of a classical electromagnetic wavepacket propagating through a piece of glass will travel at the group velocity, but it is not entirely clear that one can interpret this classical wavepacket as if it were the wavefunction of the single photon and then use the Born interpretation for this wavefunction. If this interpretation were correct, then the photon would simply travel at the group velocity in this medium. However, as Sommerfeld and Brillouin have pointed out [30], at the classical level there are at least five kinds of propagation velocities in a dispersive medium: the phase, group, energy, “signal,” and front velocities, all of which differ from one another in the vicinity of an absorption line, where there is a region of anomalous dispersion. In particular, the group velocity can become “superluminal,” i.e., faster than the vacuum speed of light, in these regions. If the photon were to travel at the group velocity in this medium, would it also travel “superluminally”? If not, then at which of these velocities does the photon travel in dispersive media? (These questions become especially acute in media with inverted populations, where off-resonance wavepackets can travel superluminally without attenuation and with little dispersion [31]; see also the accompanying article by Chiao et al.)

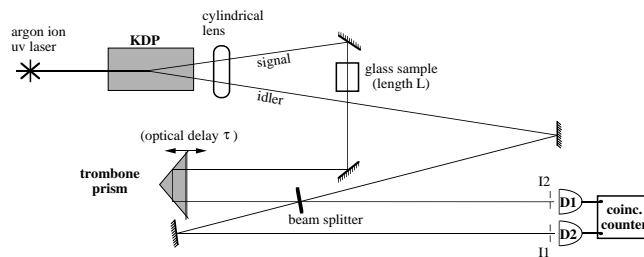


FIG. 17. Dispersion cancellation schematic for measuring photon propagation times: a Hong-Ou-Mandel apparatus with glass sample inserted.

Motivated by the above questions, we did the following experiment. We removed the HWP and the polarizers from the quantum eraser setup and inserted a piece of glass in the path of one of the photons; see Fig. 17. The glass slows down the photon which traverses it, and in order to observe the coincidence dip, it is necessary to introduce an equal, compensating delay τ by adjusting the trombone prism. We measured the magnitude of this delay for various samples of glass and were able to determine traversal times on the order of 35 ps, with ± 1 fs accuracy. In this way, we were able to confirm that single photons travel through glass at the group velocity in transparent spectral regions, an interesting example of particle-wave unity.

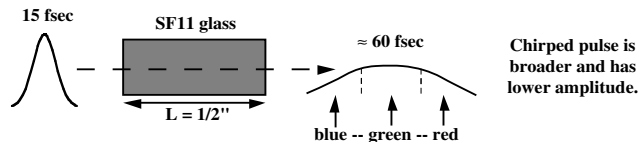


FIG. 18. Chirped pulse due to normal dispersion

Clearly, the interest of measuring optical delays is greatest for media with dispersion. Consider the limiting time-resolution of this interferometer. For a short wavepacket or pulse, a broad spectrum is necessary. In dispersive media, however, the broad spectrum required for an ultrafast pulse (or single-photon wavepacket) can lead to a great deal of dispersion. One might expect that this broadening of the wavepacket would also broaden the coincidence dip in the HOM interferometer, since the physical explanation of the dip (in terms of which-path information carried by the photons’ arrival times) seems to imply that the width of the dip should be the size of the wavepackets which impinge on the beam splitter. Thus the tradeoff between pulse width and dispersive broadening would place an ultimate limit on the resolution of a measurement made on a given sample. For example, a 15 fs wavepacket propagating through half an inch of SF11 glass (one of the samples we studied) would classically broaden to about 60 fs due to the dispersion in this glass. The nature of the broadening is that of a chirp, i.e., the local frequency sweeps from low to high values (for normal dispersion, in which redder wavelengths travel faster than bluer wavelengths). Hence the earlier part of the broadened pulse consists of redder wavelengths, and the later part of this pulse consists of bluer

wavelengths; see Fig. 18.

In our experiment, however, we found that the combination of the time-correlations and energy-correlations exhibited by our entangled photons led to a cancellation of these dispersive effects. While the individual wavepacket which travels through the glass does broaden according to classical optics, it is impossible to know whether this photon was reflected or transmitted at the beam splitter (recall Fig. 12). This means that when an individual photon arrives at a detector, it is unknowable whether it travelled through the glass or whether its conjugate (with *anticorrelated* frequency) did so; due to the chirp, the delay in these two cases is opposite, relative to the peak of the wavepacket. An exact cancellation occurs for the (greatly dominant) linear group-velocity dispersion term, and no appreciable broadening of the 15 fs interference dip occurs. This is a direct consequence of the nature of the EPR state, in that it relies on the simultaneous correlations of energy and time. A detailed theoretical analysis predicted these results, in agreement with the simple argument presented here [32].

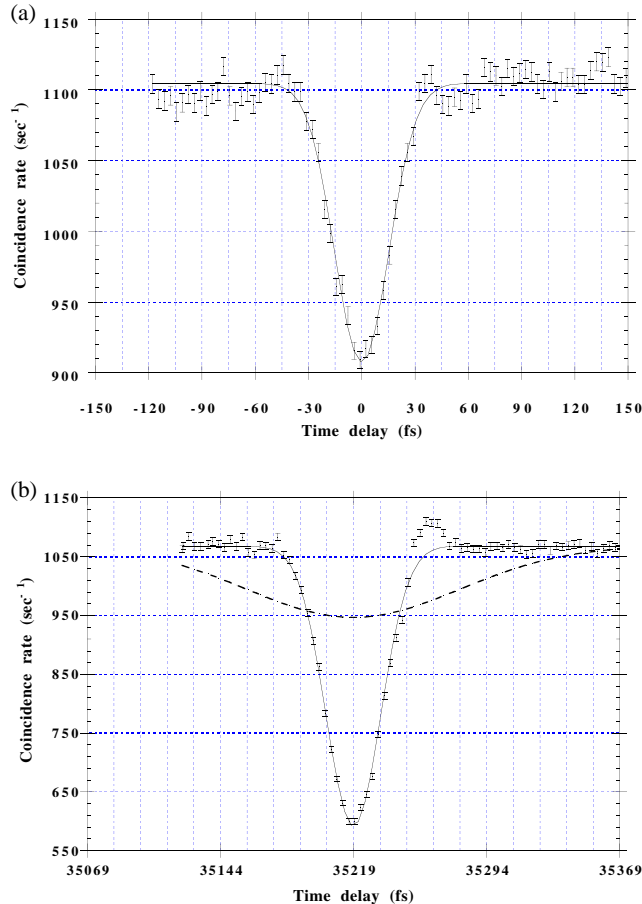


FIG. 19. HOM coincidence rate as a function of the relative optical time delay in the interferometer. (a) The solid line is a Gaussian fit, with an rms width of 15.3 fs. (b) Coincidence profile after a $\frac{1}{2}$ -inch piece of SF11 glass is inserted in the signal arm of the interferometer. The dip shifts by 35,219 fs, but no broadening is observed. Classically, a 15-fs pulse would broaden to at least 60 fs, shown for comparison as a dashed line.

In Fig. 19, we see that there is indeed very little broadening in the data with the glass compared with that without the glass. Certainly, broadening on the scale of 60 fs (the dashed curve) is ruled out by these data. Dispersion cancellation is important for applications; particularly, in the tunneling-time measurements described next, the sharpness of the dip—and hence the temporal resolution—is not appreciably degraded by the presence of the dispersion in the optical elements of our apparatus or in the sample itself.

VII. MEASUREMENTS OF PHOTON TUNNELING TIMES

Tunneling is one of the most striking consequences of quantum mechanics. The Josephson effect in solid state physics, fusion in nuclear physics, and instantons in high energy physics are all manifestations of this phenomenon. Every quantum mechanics text treats the calculation of the tunneling probability. And yet, the issue of how much *time* it takes a particle to tunnel through a barrier, a problem first addressed in the 1930s, remains controversial to the present day. The question arises because the momentum in the barrier region is imaginary. The first answer, the group delay (also known as the “phase time” because it describes the time of appearance of a wavepacket peak by using the stationary phase approximation), can in certain limits be paradoxically small, implying barrier traversal at a speed greater than that of light in vacuum [33,34]. This apparent violation of Einstein causality does not arise from the use of the nonrelativistic Schrödinger equation, since it also arises in solutions of Maxwell’s equations, which are fully relativistic. It has generally been assumed that such superluminal velocities cannot be physical [30], but in the case of tunneling, no resolution has been universally accepted.

As a result of developments in solid state physics, such as tunneling in heterostructure devices, the issue has acquired a new sense of urgency since the 1980s, leading to much conflicting theoretical work [35–37]. Several experimental papers presenting more or less indirect measurements of barrier traversal times have appeared. Some seem to agree with the “semiclassical time” of Büttiker and Landauer [35,38], while others [39,40] seem to agree with the group delay (“phase time”). We presented the first direct time measurement confirming that the time delay in tunneling can be superluminal, studying single photons traversing a dielectric mirror [6]. Since then, several microwave experiments have confirmed that the effective group velocity of classical evanescent waves in various configurations may be superluminal [41–43]. Also, recently a femtosecond laser experiment has confirmed our earlier findings of superluminal tunneling in dielectric mirrors [44], using classical pulses.

Our experiment again employs the down-conversion source in a HOM interferometer arrangement. The advantage of using these conjugate particles is that after one particle traverses a tunnel barrier its time of arrival can be compared with that of its twin (which encounters no barrier), thus offering a clear operational definition and direct measurement of the time *delay* in tunneling. Since this technique relies on coincidence detection, the particle aspect of tunneling can be clearly observed: Each coincidence detection corresponds to a single tunneling event.

In our apparatus, the tunnel barrier is a multilayer dielectric mirror. Such mirrors are composed of quarter-wave layers of alternating high- and low-index materials, and hence possess a one-dimensional “photonic band gap” [45], i.e., a range of frequencies which correspond to pure imaginary values of the wavevector. They are optical realizations of the Kronig-Penney model of solid state physics, and thus analogous to crystalline solids possessing band gaps, as well as to superlattices. Our mirrors have an $(HL)^5H$ structure, where H represents titanium oxide (with an index of 2.22) and L represents fused silica (with an index of 1.41). Their total thickness d is $1.1\ \mu\text{m}$, implying a traversal time of $d/c = 3.6\ \text{fs}$ if a particle were to travel at c . Their band gaps extend approximately from 600 to 800 nm, and their transmission amplitudes reach a minimum of 1% at 692 nm.

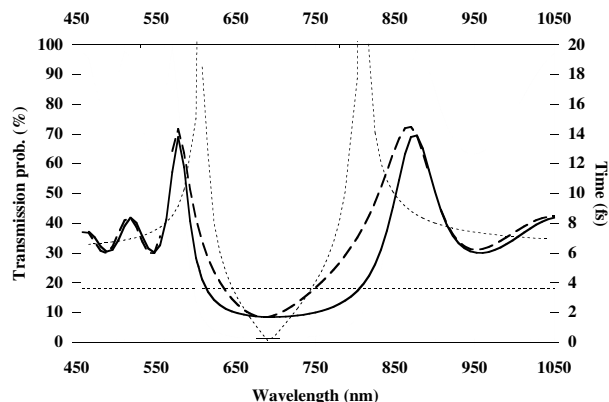


FIG. 20. Theoretical curves, where the light solid curve shows the transmission probability (left axis) of our multilayer coating, as a function of incident wavelength. The heavy solid curve shows the group delay, the heavy dashed curve shows the Büttiker-Larmor traversal time, and the light dotted curve the semiclassical time (right axis). The horizontal dotted line at 3.6 fs represents the “causality limit” d/c .

The semiclassical time is calculated from the group velocity which would hold inside an infinite periodic medium (i.e., neglecting reflections at the extremities of the barrier). As the wavevector becomes pure imaginary for frequencies

within the band gap, so does the semiclassical time; in order to extend it into the band-gap region, we simply drop the factor of i , in analogy with the interaction time of Büttiker and Landauer [35]. The “Larmor time” is a measure of the amount of Larmor precession a tunneling electron would experience in an infinitesimal magnetic field confined to the barrier region. Büttiker has suggested a Larmor time which takes into account the tendency of the transmitted electrons to align their spins *along* the magnetic field as well as the precession *about* the field [46]. The group delay is the derivative of the barrier’s transmission phase with respect to the angular frequency of the light, according to the method of stationary phase. All three times dip below $d/c = 3.6$ fs and are thus superluminal, although their detailed behaviors are quite different; see Fig. 20. For example, the group delay remains relatively constant near 1.7 fs over most of the band gap. The semiclassical time, on the other hand, dips below 3.6 fs only over a narrower range of frequencies, and actually reaches zero at the center of the gap. Büttiker’s Larmor time approaches the group delay far from the band gap as well as at its center, but differs from it at intermediate points.

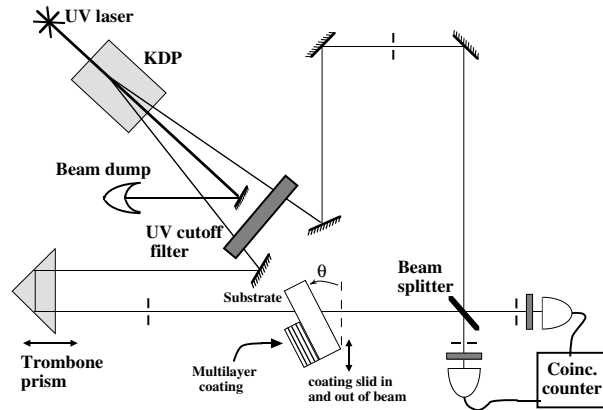


FIG. 21. Experimental setup for determining the single-photon propagation times through a multilayer dielectric mirror.

Our apparatus is shown in Fig. 21. As before, a KDP crystal is pumped by a cw uv laser at 351 nm, producing pairs of down-conversion photons, directed by mirrors to impinge simultaneously on the surface of a 50/50 beam splitter. One photon of each pair travels through air, while the conjugate photon impinges on our sample, consisting of an etalon substrate of fused silica, which is coated over half of one face with the $1.1 \mu\text{m}$ coating described above, and uncoated on the other half of that face. (The entire opposite face is antireflection coated.) This sample is mounted on two stacked stages. The first is a precision translation stage, which can place the sample in either of two positions transverse to the beam path. In one of these positions, the photon must tunnel through the $1.1 \mu\text{m}$ coating in order to be transmitted, while in the other position, it travels through $1.1 \mu\text{m}$ of air. In both positions, it traverses the same thickness of substrate. The second stage allows the sample to be tilted with respect to normal incidence.

If the two photons’ wavepackets are made to overlap in time at the beam splitter, the destructive interference effect described above leads to a theoretical null in the coincidence detection rate. Thus as the path-length difference is changed by translating a “trombone” prism with a Burleigh Inchworm system (see Fig. 21) the coincidence rate exhibits a dip with an rms width of approximately 20 fs, which is the correlation time of the two photons (determined by their 6 nm bandwidths) [24,32,47]. As explained above, the rate reaches a minimum when the two wavepackets overlap perfectly at the beam splitter. For this reason, if an extra delay is inserted in one arm of this interferometer (i.e., by sliding the $1.1 \mu\text{m}$ coating into the beam), the prism will need to be translated in order to compensate for this delay and restore the coincidence minimum. In order to eliminate so far as possible any systematic errors, we conducted each of our data runs by slowly scanning the prism across the dip, while sliding the coating in and out of the beam periodically, so that at each prism position we had directly comparable data with and without the barrier.

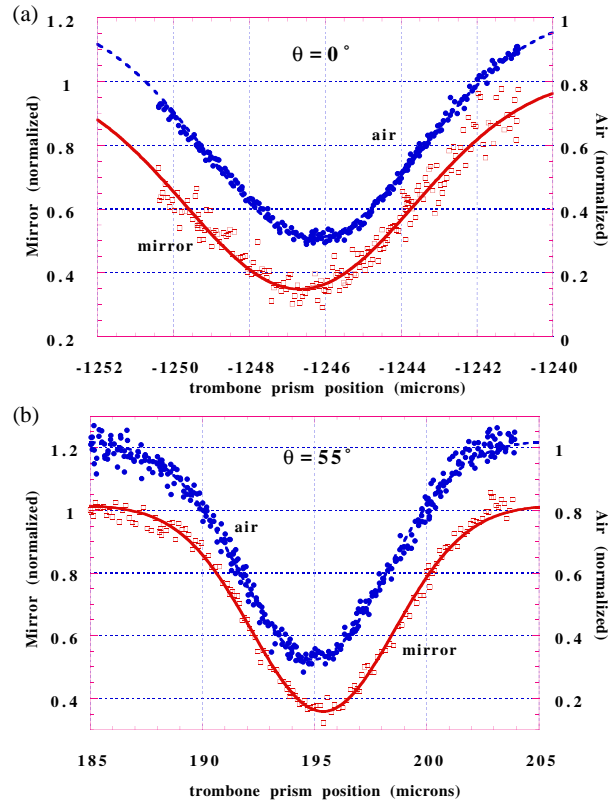


FIG. 22. This caption intentionally removed due to latex problems.

We found that inserting the barrier at normal incidence (for which it was designed) did in fact cause the dip to be shifted to a position in which the prism was located *farther* from the barrier. This determines the sign of the effect: The external delay had to be *lengthened*, implying that the mean delay time experienced by the photon inside the barrier was *less than* the delay time for propagating through the same distance in air. As we rotated the mirror about the vertical axis, the bandgap shifted to lower wavelengths according to Bragg's law, and for the p-polarized photons we studied, the width of the bandgap also diminished due to the decreased reflectivity of the dielectric interfaces at non-normal incidence (cf. Brewster's angle). Thus at 0° , our 702 nm photons are near the center of the bandgap, while at 55° , they are near the band edge, where the transmission is over 40%. As can be seen clearly from Fig. 22, the delay time changes from a superluminal value to a subluminal one as the angle of incidence is scanned, in agreement with theory.

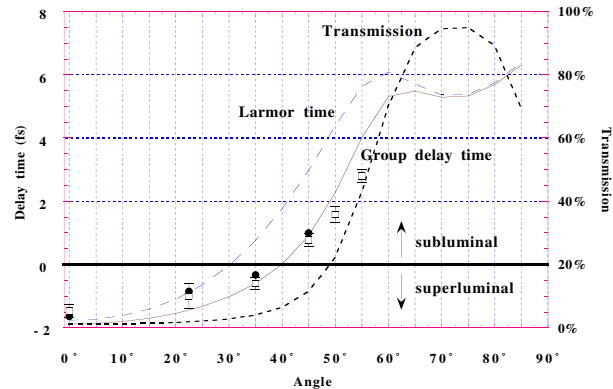


FIG. 23. Left axis: measured delay for mirror one (\square) and mirror two (\bullet) as a function of angle of incidence, to be compared with the theoretical group delay and the Larmor interaction time proposed by Büttiker. Right axis: transmission versus angle of incidence. All curves are for p-polarization.

Our normal-incidence data [6] demonstrated that the semiclassical time was inadequate for describing these prop-

agation delays, and the data were roughly consistent both with the group delay theory and with Büttiker’s proposed Larmor time [46]. More recent data [7] is summarized in Fig. 23. As can be seen, the evidence for a superluminal delay which becomes subluminal as the photons approach the band edge is quite convincing. There is reasonable agreement with the group delay theory, although a discrepancy on the order of one-half a femtosecond (and greater at large angles of incidence) remains; we believe this may be attributable to deviations from an ideal barrier, such as varying layer thicknesses and residual absorption or scattering. While the discrepancy is not yet fully understood, the data for two different mirrors we studied (both shown in the figure) demonstrate clearly that the observable delay time is better described by the group delay theory than by the Larmor time.

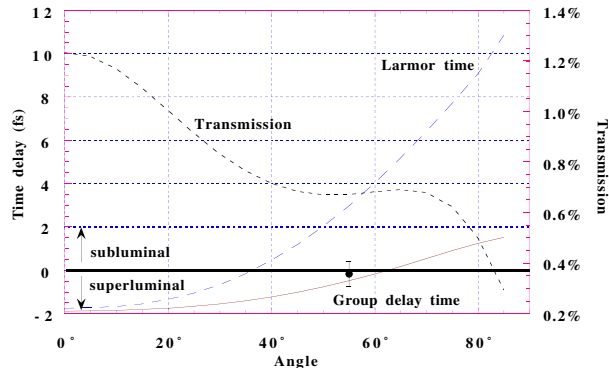


FIG. 24. Same as Fig. 23, but for s-polarization. Due to the much lower transmission, only one preliminary data point is shown, but the different characteristics of the theoretical curves for both transmission and delay suggest that upon improvement of our signal-to-noise ratio, further work in this direction may help elucidate the discrepancy between experiment and theory (as well as to more conclusively rule out identification of the Larmor time as descriptive of the measured delay).

In order to study this discrepancy, in addition to obtaining a second mirror of the same design parameters, we have begun to measure the delay times for s-polarization, for which the interface reflectivities increase with angle, making the bandgap wider instead of narrower. A preliminary data point is shown in Fig. 24, along with theoretical curves which demonstrate both why this should be an interesting avenue for further investigation and why it is more difficult to get an adequate signal-to-noise ratio. The point shown is consistent with the group delay, and not with the Larmor time.

We have thus confirmed that the peak of a tunneling wave packet may indeed appear on the far side of a barrier sooner than if it had been travelling at the vacuum speed of light. No signal can be sent with these smooth wavepackets, however; only a small portion of the leading edge of the incident Gaussian is actually transmitted, and whether the photon “collapses” into this portion or into the reflected portion is not under experimental control. Causality is thus not violated by these nonlocal effects. The superluminality can be understood by thinking of the low transmission through our barrier as arising from destructive interference between waves which have spent different lengths of time in the barrier. While the incident wavepacket is rising, multiple reflections can be neglected, since their intensities are small relative to the partial wave which makes a single pass; thus the destructive interference is not very effective. At later times, when the fields stored in the barrier have had time to reach a steady state, the interference reduces the transmission to its steady-state value. Thus the leading edge of the packet is transmitted preferentially with respect to the rest of the packet, shifting the transmitted peak earlier in time.

Recent work based on “weak measurement” theory [48] and the idea of conditional probability distributions for the position of a quantum particle suggests that this superluminal effect is related to the fact that a tunneling particle spends very little time in the barrier region, except within an evanescent decay length of the two barrier edges [49–51]. It is as though the particle “skipped” the bulk of the barrier. Furthermore, the nonlocality is underscored by the fact that this approach allows one to describe conditional probability distributions for a particle which is first prepared incident on the left and later detected emerging on the right. These probability distributions describe in-principle measurable effects, and do indeed traverse the barrier faster than the vacuum speed of light. They suggest that a single tunneling particle could affect the expectation values of two different measuring devices located at spacelike separated positions, so long as the coupling to the devices was too weak to disturb the tunneling process, and hence too weak to shift either measuring device by an amount comparable to its intrinsic uncertainty.

VIII. CONCLUSION

The experiments which we have described in this paper demonstrate some of the stranger nonlocal features of quantum mechanics. The first three of these experiments explore them in connection with the Einstein-Podolsky-Rosen effect. In the Franson experiment, the behaviors of the two space-like separated particles at the final beam splitters (i.e., which exit port they choose) are correlated or anticorrelated with each other, depending on the settings of the phase shifters in the interferometer. Likewise, in the quantum eraser, whether interference or the complementary which-path information is observed can be controlled by the experimenter's choice of the settings of polarizers placed after the final beam splitter of the interferometer. In the dispersion cancellation experiment, one cannot know, even in principle, which of two photons propagated through a piece of the glass. This in turn leads to a cancellation of the effect of dispersive broadening on the measurement. The fourth of these experiments shows that, even at the one-particle level, there exist nonlocal effects in quantum mechanics: in tunneling there exist superluminal time delays of the tunneling particle. None of these nonlocal effects violates Einstein causality, due to the uncontrollable randomness of quantum events. In the fourth experiment, there is another way to understand that Einstein causality is not violated; the front velocity, at which *discontinuities* propagate, never exceeds c (see accompanying article by Chiao *et al*).

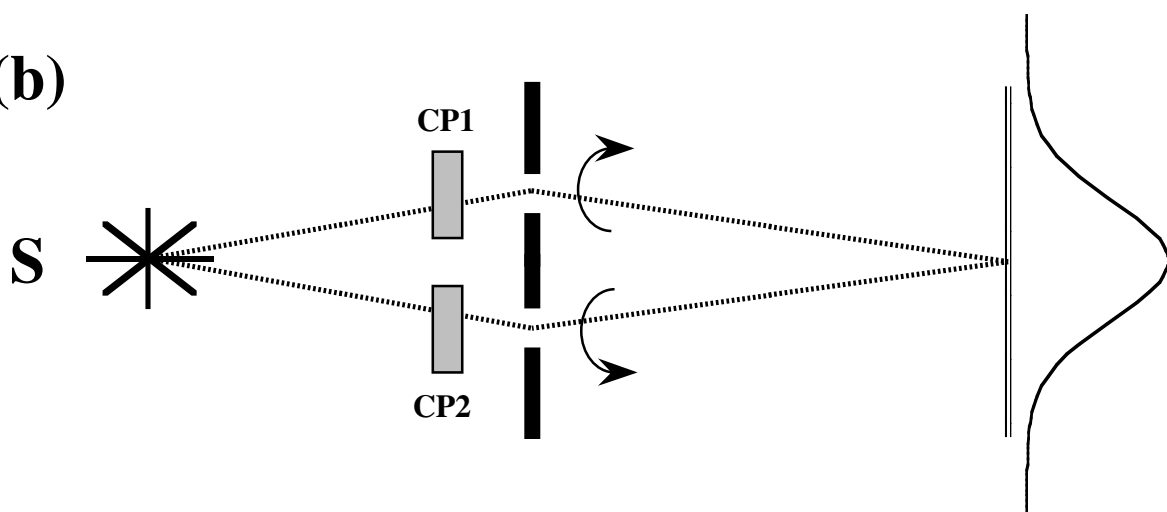
IX. ACKNOWLEDGMENTS

We would like to thank Jack Boyce, Jeff Chamberlain, Josh Holden, Bruce Johnson, Grant McKinney and Morgan Mitchell for their assistance in the tunneling time experiment and preparation of this manuscript, and Winfried Heitmann for helpful e-mail. RYC would like to thank Prof. S. Zubairy for an invitation to speak at the '94 summer school in Nathiagali, Pakistan at which these results were presented. This work was supported by ONR grant number N00014-90-J-1259.

-
- [1] Einstein A, Podolsky B and Rosen N 1935 *Phys. Rev.* **47** 777
 - [2] Franson J D 1989 *Phys. Rev. Lett.* **62** 2205
 - [3] Kwiat P G, Steinberg A M and Chiao R Y 1993 *Phys. Rev. A* **47** R2472
 - [4] Kwiat P G, Steinberg A M and Chiao R Y 1992 *Phys. Rev. A* **45** 7729
 - [5] Steinberg A M, Kwiat P G and Chiao R Y 1992 *Phys. Rev. Lett.* **68** 2421
 - [6] Steinberg A M, Kwiat P G and Chiao R Y 1993 *Phys. Rev. Lett.* **71** 708
 - [7] Steinberg A M and Chiao R Y 1994 *Phys. Rev.* Submitted (quant-ph/9501013) *Sub-femtosecond determination of transmission delay times for a dielectric mirror (photonic bandgap) as a function of angle of incidence*
 - [8] Bohm D 1983 in *Quantum Theory and Measurement* ed J A Wheeler and W H Zurek (Princeton: Princeton) p 356
 - [9] Freedman S J and Clauser J F 1972 *Phys. Rev. Lett.* **28** 938
 - [10] Clauser J F and Shimony A 1978 *Rep. Prog. Phys.* **41** 1881
 - [11] Aspect A, Dalibard J and Roger G 1982 *Phys. Rev. Lett.* **49** 1804
 - [12] Bell J S 1964 *Physics* **1** 195
 - [13] Rarity J G and Tapster P R 1990 *Phys. Rev. Lett.* **64** 2495
 - [14] Schrödinger E 1983 in *Quantum Theory and Measurement* ed J A Wheeler and W H Zurek (Princeton: Princeton) p 152
 - [15] Chiao R Y, Kwiat P G and Steinberg A M 1991 *Proceedings Workshop on Squeezed States and Uncertainty Relations* ed D Han, Y S Kim and W W Zachary (NASA Conference Publication 3135) p 61
 - [16] Brendel J, Mohler E and Martienssen W 1992 *Europhys. Lett.* **20** 575
 - [17] Rarity J G and Tapster P R 1994 *Phys. Rev. Lett.* **73** 1923
 - [18] Clauser J F, Horne M A, Shimony A and Holt R A 1969 *Phys. Rev. Lett.* **23** 880
 - [19] Kwiat P G 1993 *Nonclassical Effects from Spontaneous Parametric Down-Conversion: Adventures in Quantum Wonderland* PhD thesis (U C Berkeley)
 - [20] Scully M O, Englert B -G and Walther H 1991 *Nature* **351** 111
 - [21] Feynman R P, Leighton R B and Sands M 1965 *The Feynman Lectures on Physics* (Reading, MA: Addison-Wesley) **III** 3-5
 - [22] Stern A Aharonov Y and Imry Y 1990 *Phys. Rev. A* **41** 3436
 - [23] Jordan T F 1993 *Phys. Rev. A* **48** 2449

- [24] Hong C K, Ou Z Y and Mandel L 1987 *Phys. Rev. Lett.* **59** 2044
- [25] Steinberg A M and Chiao R Y 1994 *Phys. Rev. A* **49** 3283
- [26] Shih Y H and Alley C O 1988 *Phys. Rev. Lett.* **61** 2921
- [27] Ou Z Y and Mandel L 1988 *Phys. Rev. Lett.* **61** 50
- [28] Wheeler J A 1983 in *Quantum Theory and Measurement* ed J A Wheeler and W H Zurek (Princeton: Princeton) p 182
- [29] Kwiat P G, Steinberg A M and Chiao R Y 1994 *Phys. Rev. A* **49** 61
- [30] Brillouin L 1960 *Wave Propagation and Group Velocity* (New York: Academic Press)
- [31] Chiao R Y 1993 *Phys. Rev. A* **48** R34
- [32] Steinberg A M, Kwiat P G and Chiao R Y 1992 *Phys. Rev. A* **45** 6659
- [33] MacColl L A 1932 *Phys. Rev.* **40** 621
- [34] Wigner E P 1955 *Phys. Rev.* **98** 145
- [35] Büttiker M and Landauer R 1982 *Phys. Rev. Lett.* **49** 1739
- [36] Hauge E H and Støvneng J A 1989 *Rev. Mod. Phys.* **61** 917
- [37] Landauer R and Martin T 1994 *Rev. of Mod. Phys.* **66** 217
- [38] Landauer R 1989 *Nature* **341** 567
- [39] Landauer R 1993 *Nature* **365** 692
- [40] Støvneng J A and Hauge E H 1993 *Phys. World* **6** 23
- [41] Enders A and Nitz G 1993 *J. Phys. I* **3** 1089
- [42] Nitz G, Enders A and Spieker 1994 *J. Phys. I* **4** 565; Steinberg A M 1994 *J. Phys. I* **4** 1813
- [43] Ranfagni A, Fabeni P, Pazzi G P, and Mugnai D 1993 *Phys. Rev. E* **48** 1453
- [44] Spielmann Ch, Szpöcs R, Stigl A and Krausz F 1994 *Phys. Rev. Lett.* **73** 2308
- [45] Yablonovitch E and Leung K M 1991 *Physica* **175B** 81 and references therein
- [46] Büttiker M 1983 *Phys. Rev. B* **27** 6178
- [47] Jeffers J and Barnett S M 1993 *Phys. Rev. A* **47** 3291
- [48] Aharonov Y and Vaidman L 1988 *Phys. Rev. Lett.* **58** 1351
- [49] Steinberg A M 1994 *Phys. Rev. Lett.* submitted (quant-ph/9501015) *How much time does a tunneling particle spend in the barrier region?*
- [50] Steinberg A M 1994 *Phys. Rev. A* submitted *Conditional probabilities in quantum theory, and the tunneling time controversy*
- [51] Steinberg A M 1994 *When Can Light Go Faster Than Light? The tunneling time and its sub-femtosecond measurement via quantum interference* PhD thesis (U C Berkeley)

(b)



(c)

